Responses to climatic changes since the Little Ice Age on Maladeta Glacier (Central Pyrenees)

J. Chueca Cía[a], A. Julián Andrés[b], M.A. Saz[b], J. Creus Novau[c], J.I. López Moreno[d]

[a]*Departamento de Geografía, Facultad de Ciencias Humanas y de la Educación, Universidad de Zaragoza, 22002-Huesca, Spain*
[b]*Departamento de Geografía, Facultad de Filosofía y Letras, Universidad de Zaragoza, 50009-Zaragoza, Spain*
[c]*Instituto Pirenaico de Ecología, CSIC, Campus de Jaca (Huesca), Spain*
[d]*Instituto Pirenaico de Ecología, CSIC, Campus de Aula Dei, 50080-Zaragoza, Spain*

Abstract

The evolution of Maladeta Glacier (Maladeta massif, central Spanish Pyrenees) since the Little Ice Age maximum is analyzed in this work. The extent of the glacier was mapped into 10 stages using morainic deposits and graphic documents. Climatic data (temperature and precipitation) were reconstructed by using dendroclimatic techniques complemented by recent instrumental records. The results thus obtained confirm the control of the above mentioned climatic factors, particularly annual temperature and winter precipitation, in the evolution of Maladeta Glacier, which has receded from an extent of 152.3 ha in 1820–1830 to 54.5 ha in 2000, a 35.7% reduction in size. The rate of ice wastage has varied during that period, defining several phases of glacial stabilization (1820–1830 to 1857; 1914–1920 to 1934–1935; 1957 to 1981), moderated glacial depletion (1901–1904 to 1914–1920; 1934–1935 to 1957) and marked glacial depletion (1857 to 1901–1904; 1981 to 2000). The evolution of Maladeta Glacier is also in keeping with trends observed from other alpine Mediterranean glaciers, which have experienced a consistent rise in their equilibrium line altitudes during the 19th and 20th centuries as well as associated and prolonged periods of negative mass balance

Keywords: Deglaciation, Little Ice Age, Climatic changes, Maladeta Glacier, Pyrenees

1. Introduction

The deglaciation process recorded by Pyrenean glaciers since the end of the Little Ice Age (LIA) has been analyzed in several works (Martínez de Pisón and Arenillas, 1988; Gellatly et al., 1995; Copons and Bordonau, 1997; Julián and Chueca, 1998; Chueca

and Julián, 2002; Chueca et al., 2002). In this paper, we present a detailed reconstruction of the glacier retreat observed in the Maladeta Glacier (Maladeta massif; central Spanish Pyrenees) and examine the relationship between that evolution and climatic fluctuations. Using different sources of data (morainic deposits, graphic documents), the extent of the glacier has been reconstructed and mapped into ten stages constrained by reliable chronological data (1820–1830; 1857; 1876; 1901–1904; 1914–1920; 1934–1935; 1957; 1981; 1990; 2000). This information is compared with basic climatic data (temperature and precipitation), reconstructed for the same geographical area for that period by using dendroclimatic techniques and complemented by recent instrumental records of several South-Pyrenean weather stations.

2. Study area

The Maladeta massif has today the best preserved and largest glacial remnants in the whole Pyrenean region. The massif is located between the Ésera and Noguera Ribagorzana valleys (Fig. 1), and is formed of crystalline rocks of the Maladeta batholith. This igneous body extends in an E–W direction and consists of homogenous masses of granodiorite and granite. The massive nature and resistance of these materials confers to the area its particular morphology and high altitudes (Aneto, 3404 m; Maladeta, 3308 m). The topographical NW–SE disposition of the massif has determined, as in the case of other Pyrenean glaciated sectors such as Infiernos, Vignemale or Monte Perdido, the development and conservation of several north–northeast-facing cirque glaciers which cover today an area of 197.2 ha. The largest glacial bodies are Aneto (90.4 ha), Maladeta Oriental (48.4 ha), Tempestades Occidental (14.3 ha), Barrancs (10.8 ha) and Maladeta Occidental (6.1 ha) (Chueca et al., 2002).

The total extent of ice measured in the massif today represents 32% of the total present (616.2 ha) during the Final Stage of the LIA, dated to around 1820–1830 (Chueca and Julián, 1996). Maladeta Glacier (Fig. 2) has recently been fragmented into two separate bodies, Maladeta Occidental and Maladeta Oriental glaciers but, during the LIA maximum, the single Maladeta Glacier had a surface of 152.3 ha. In spite of the noticeable reduction in extent and thickness, both glaciers still exhibit an appreciable dynamism, with development of longitudinal and transversal crevasses of several meters width and depth. The geophysical investigations carried out by Martínez and García (1994) and Martínez et al. (1997) detected ice-thicknesses slightly over 50 m in the case of the Maladeta Oriental glacier (located in its easternmost proximal section) and over 30 m in the Maladeta Occidental glacier (in its westernmost

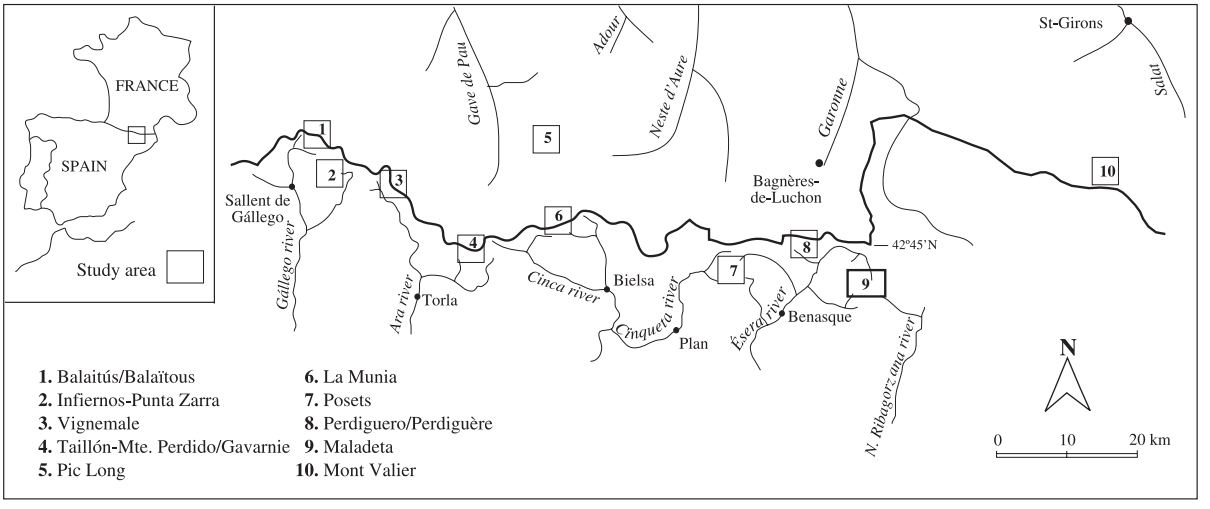

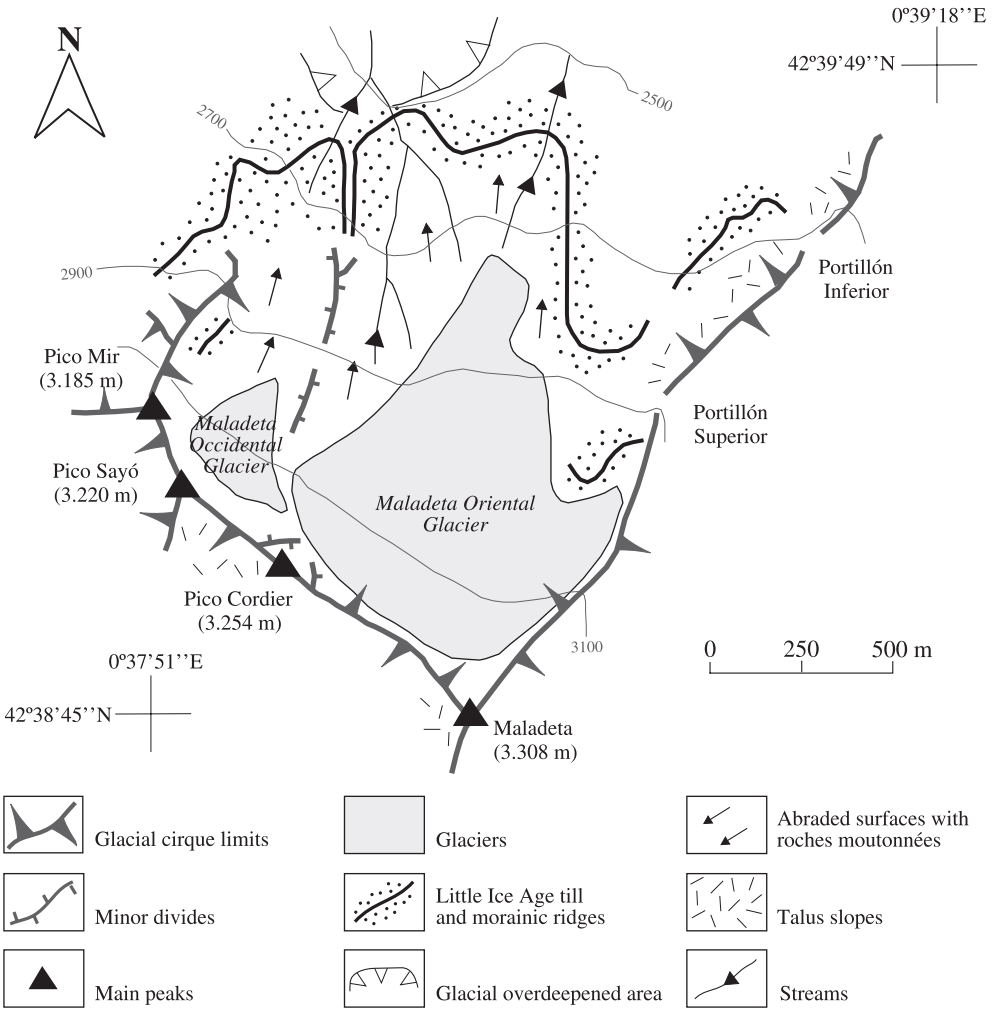

proximal section). The equilibrium line altitude (ELA) in the area is positioned at approximately 3000–3100 m a.s.l. (Chueca and Julián, 1994).

3. Methods

3.1. Reconstruction of glacial evolution

The reconstruction of the evolution of Maladeta Glacier (Fig. 3) is based on the methodology adopted in a previous study of the nearby Coronas Glacier (Chueca et al., 2003). As a starting point of reference, we used the maximum extent reached by the Maladeta Glacier during the LIA, dated from its morainic deposits to around 1820–1830 (Chueca and Julián, 1996). For the other nine stages, we examined and/or used different graphic sources whenever they presented sufficient reliability:

1) *iconography* (engravings, drawings): Although they have not directly been used in the cartography of the glacier extent, they were consulted as support for other documents. Iconographic sources include drawings of the north slope of the massif by Friedrich Parrot around 1820 (Parrot, 1823), engravings from around 1850–1860 made by lithographer Victor Petit for the *Guide Joanne*

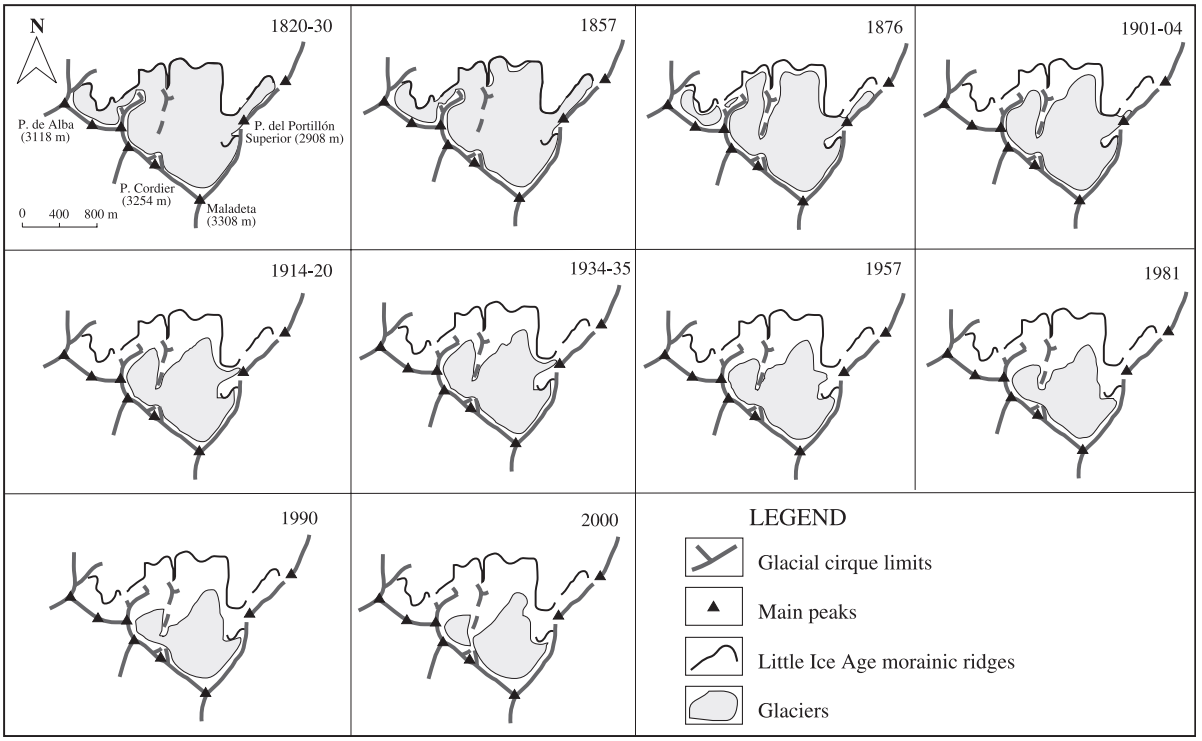

Fig. 3. Cartography of Maladeta Glacier evolution through the ten analyzed stages.

(Joanne, 1862), and a lithography from 1856 by Edouard Paris.

2) *topographic maps*: Different Spanish and French editions exist for the zone. Their scale (mainly 1:50.000), makes the reliability of the ice cartography very low. Additionally, most of these topographic documents cover only the second half of the 20th century, a period for which more precise sources are available. Two remarkable exceptions, used as supporting documents, are the mapping surveys carried out by Charles Packe and Franz Schrader in the Maladeta massif around 1867 and 1890, respectively (Packe, 1867; Schrader, 1894).
3) *aerial photographs*: Once georectified, these documents are highly reliable. In this study we have used the 1957 aerial survey (American flight; August 1957; scale 1:30.000; black and white), 1981 aerial survey, hampered by the presence of a more extensive snow cover (South Pyrenees flight; September 1981; scale 1:25.000; black and white) and 1997–2000 aerial survey (Aragonese Government flight; August–September 1997–2000; scale 1:20.000; colour).
4) *terrestrial photographs*: If the places from which the photographs were taken are the same, and the images are significant (include the whole or a major part of the glacier and show a reduced amount of snow), they are very useful documents. A serious problem is their correct dating, particularly with the oldest documents. The photographs used in our study are, therefore, only those significant and for which a trustworthy chronology has been established (Chueca and Julián, 2002). The number of old documents of this kind available for the north slope of the Maladeta massif, and used in our reconstructions, is considerable, and includes photographs by A. Civiale (1857), E. Trutat (1876), J. Soler Santaló (1901), L. Le Bondidier (1904), Catalana de Gas y Electricidad (1914), C. Lana Sarrate (1920), R. Compairé (1934) and L. García Sainz (1935). For the last three decades, the number of available photographs increases and we have used several

documents from our particular collection and from the data base of the research project "Estudio de la dinámica de los glaciares del Pirineo aragonés", that has coordinated glaciological investigations in the area since 1992. All the terrestrial photographs used in the reconstruction of the glacier have been georeferenced visually, using different terrain elements as reference points (moraines, scarps, visible bedrock features, etc.). It must be noted that there is a potential error in the georeferencing of some of the documents, particularly in the few cases where not all the perimeter of the glacier is entirely visible. We believe, in any case, that this does not affect the overall consistency of the results.

3.2. Climatic data: dendroclimatic reconstructions and instrumental data

To evaluate climatic influences on the Maladeta Glacier deglaciation process, dendroclimatic reconstructions of temperature and precipitation series in the locality of Capdella were used from the beginning of 19th century until the 1950s, when instrumental records are available for the area. Capdella is located 35 km to the east of Maladeta Glacier, at 1485 m a.s.l. in the southern area of the Aigües Tortes and Sant Maurici National Park (Fig. 4). The quality of the climatic data from this weather station, without urban effects or statistically significant inhomogeneities, makes its temperature and precipitation data especially adequate to carry out reconstructions using dendroclimatic techniques. Additionally, regional temperature and precipitation data obtained from recent instrumental records of several South-Pyrenean weather stations located between 15 and 30 km from Maladeta Glacier, were used to complement the dendroclimatic series (Fig. 4).

(1) In the dendroclimatic reconstruction of the climatic data from Capdella, five chronologies constructed in the Spanish slope of the Pyrenees were used: Aigües Tortes and Larra, obtained from *Pinus uncinata* R. samples, and Pinobajo, Trapa and Ibonciecho, from *Pinus sylvestris* L. These chronologies come from the Spanish Dendrochronological Data Bank, made up of 47 chronologies distributed throughout the country (Creus and Fernández, 1992; Creus et al., 1992). As a whole, this data bank

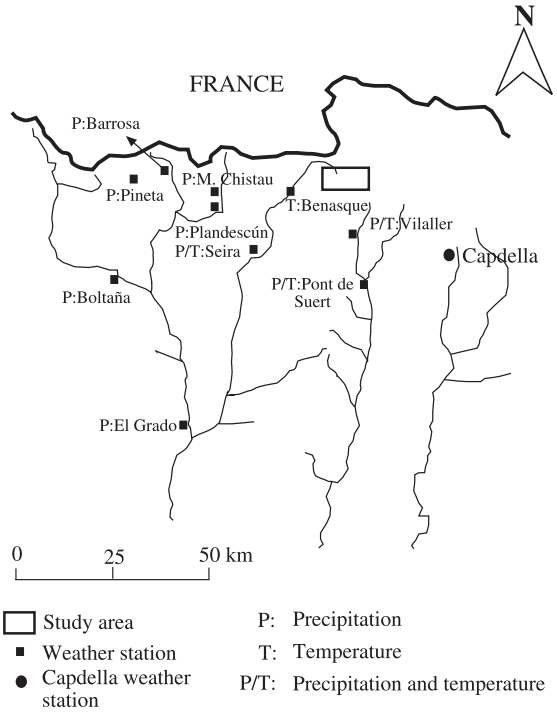

Fig. 4. Location of Capdella weather station and the observatories from which the instrumental regional series has been obtained.

contains more than 1500 samples extracted from different living trees.

Standard techniques were applied for the sampling, construction of chronologies and reconstruction of climatic variables (Fritts, 1990, 1991; Cook and Kairiukstis, 1990; Guiot, 1990). Between 20 and 25 samples were extracted from living trees to construct each chronology. Tree-rings widths were measured with a resolution of 0.01 mm using an ANIOL measuring table connected to a PC and the program CATRAS (Aniol, 1983). Absolute dating of tree-rings was checked by program COFECHA (Holmes, 1997). This software makes it possible to detect and correct false or missing rings and measure errors. ARSTAN program was used to standardize ring-width measurement in order to eliminate low frequency non-climatic signals and to combine standarized indices into site chronologies (Cook and Kairiukstis, 1990). Finally, using PRECON software (Fritts and Shaskin, 1995) chronologies and climatic data were calibrated in order to obtain a response function. When a statistically significant relationship is found, a transfer function is obtained and a linear regression equation

used to reconstruct past variations in the climate from past variations in ring-widths (Fritts, 1990; Guiot, 1990). The variance explained (r^2) by each transfer function must be greater than 0.32 (Fritts, 1990, 1991); in our case, the values of r^2 calculated were 0.73 for the third trimester temperature, 0.68 for annual temperature, 0.64 for first trimester precipitation and 0.77 for annual precipitation.

(2) Instrumental data from several weather stations located in the Cinca, Ésera and Noguera Ribagorzana basins were also used to obtain recent regional series of precipitation and temperature to complement the dendroclimatic data (Fig. 4). Specifically, the precipitation series was developed from the weather stations of El Grado, Boltaña, Pineta, Barrosa, Seira, Plandescún, Molino de Chistau, Pont de Suert and Vilaller. The temperature series was made using the information collected at Benasque, Seira, Villanova, Pont de Suert and Vilaller. All data sets were at least twenty years long into the considered reference period (1951–

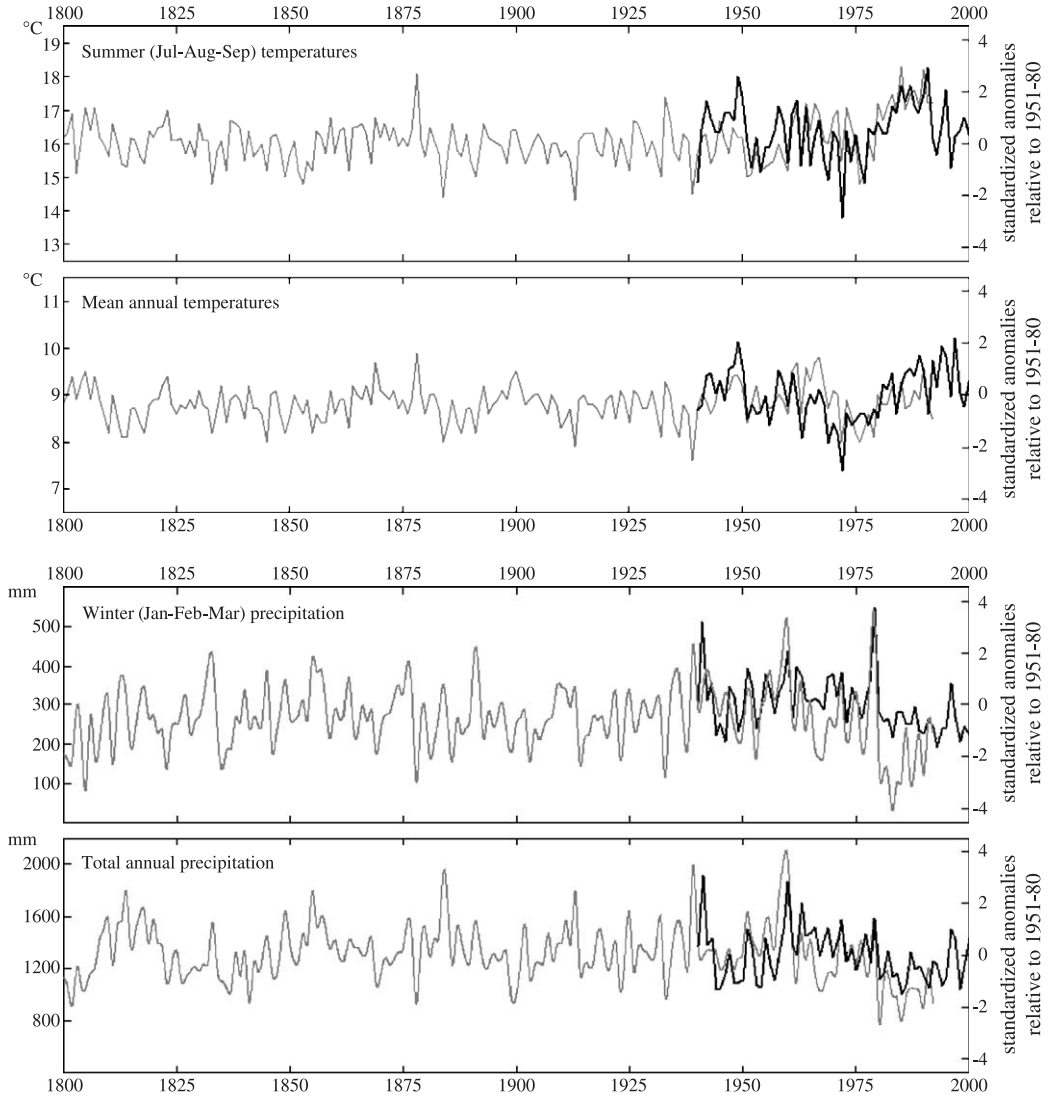

Fig. 5. Climatic data reconstructed by dendroclimatic techniques in Capdella weather station (gray line) and regional series obtained from instrumental information (black line).

1980). Missing data were filled by applying linear regression with the nearest weather stations. The regional indexes were developed in three steps: i) normalization for the series of each station by subtracting the 1951–1980 mean from the annual value and dividing by the 1951–1980 standard deviation; ii) calculation of the yearly averages of each variable of the stations that were well correlated (r^2>0.7 for rainfall, and r^2>0.6 for temperature); and iii) normalization of the averaged time series. The results were indexes that summarized well the trends for temperature and precipitation for the study area from the 1950s until 2000.

Dendroclimatic and instrumental data were grouped in quarterly values [third trimester temperature (July, August and September) and first trimester precipitation (January, February and March)] and annual values. These periods (particularly summer temperature and winter precipitation) were selected according to their impact on the glacier mass balance: summer temper-

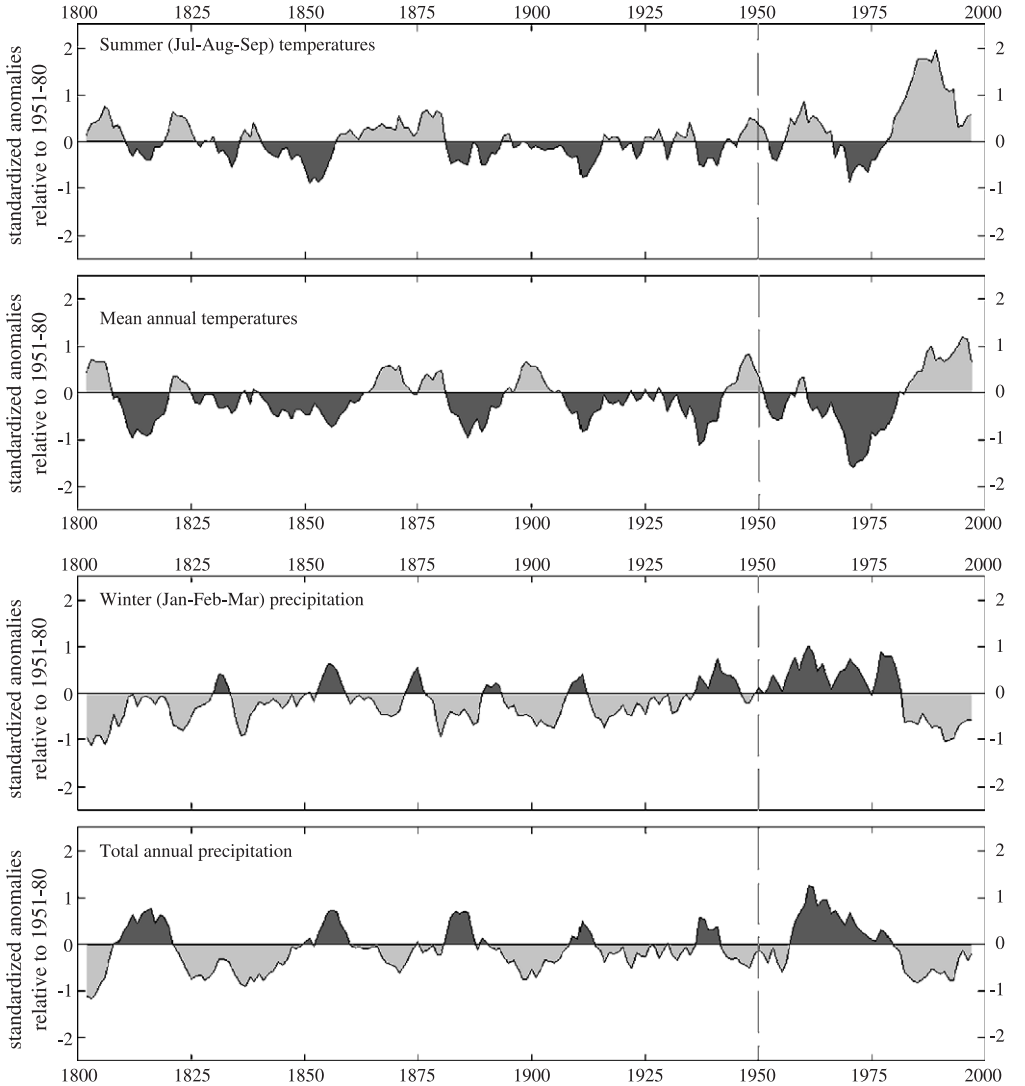

Fig. 6. Climatic data filtered with a 5 year moving average. Dendroclimatic reconstruction from Capdella weather station is used until 1950; from 1950, the regional series obtained from instrumental information is used.

Table 1
Correlation coefficients obtained between Capdella dendroclimatic series and the regional instrumental ones

	T3 instrumental	TA instrumental	P1 instrumental	PA instrumental
T3 dendroclimatic	0.60	–	–	–
TA dendroclimatic	–	0.44	–	–
P1 dendroclimatic	–	–	0.65	–
PA dendroclimatic	–	–	–	0.53

T3: average temperature of the third trimester; TA: annual mean temperature; P1: total precipitation of the first trimester; PA: annual total precipitation.

ature controls the melting–ablation conditions of the glacier; winter precipitation represents the season where the glacier receives the most important snowfalls which feed the system. The selected values are plotted in Figs. 5 and 6. The total time length of the original dendroclimatic reconstruction series for Capdella covers almost six centuries, starting in the 15th century (Saz and Creus, 2001; Saz, 2003) but, as mentioned, only data from 1800 are used on this work. From the 1950s, instrumental data were selected and used in the analysis and interpretation of the deglaciation process. Dendroclimatic and regional-instrumental series show a similar sequence during the selected common period (1940–1992) (Fig. 5). The correlation existing between dendroclimatic and instrumental data, calculated for each of the four analyzed variables (Table 1), is statistically significant in all cases (α=0.01).

4. Results and discussion

Around 1820–1830, Maladeta Glacier reached its maximum LIA superficial extent. Since that time, the glacier has experienced an almost continuous deglaciation process, especially evident in the second half of the 19th century and in the last two decades of the 20th century. In examining the relationship between glacier evolution and climatic changes, is important to note the obvious mismatch between our two data sets, continuous in the case of temperature and precipitation records, but intermittent for glacier extent (even if the amount of graphic documents we have used to reconstruct the glacial extent is considerable).

4.1. LIA maximum (1820–1830)

The maximum extent of the Maladeta Glacier has been dated from its morainic deposits (Figs. 2 and 3) at c. 1820–1830 (Chueca and Julián, 1996). The glacier was then a remarkable ice body of 152.3 ha (the area data cited in this work are planimetric surface area values; therefore, the actual surface area is likely to be slightly larger). Its length reached 1560 m, with maximum and minimum altitudinal levels of the ice mass placed at 3220 and 2510 m a.s.l., respectively. The ELA, estimated by the classic

Table 2
Basic characteristics of Maladeta Glacier in the analyzed stages

	1820–1830	1857	1876	1901–1904	1914–1920	1934–1935	1957	1981	1990	2000
Surface area (ha)	152.3	148.5	129.9	100.7	92.9	89.7	74.2	70.9	61.6	M.Oc: 6.1 M.Or: 48.4
% Surface to initial surface	100	97.5	85.2	66.1	60.9	58.8	48.7	46.5	40.4	35.7
Surface-loss rate (ha year^{-1})		−0.11	−0.97	−1.03	−0.55	−0.18	−0.68	−0.13	−1.03	−0.88
Maximum altitude (m a.s.l.)	3.220	3.220	3.220	3.200	3.200	3.200	3.200	3.200	3.200	M.Oc: 3.180 M.Or: 3.200
Minimum altitude (m a.s.l.)	2.510	2.510	2.570	2.640	2.660	2.670	2.700	2.710	2.730	M.Oc: 2.910 M.Or: 2.740
Maximum length (m)	1.560	1.540	1.540	1.540	1.340	1.300	1.220	1.200	1.100	M.Oc: 380 M.Or: 1.030
ELA (m a.s.l.)	2.840	2.840	2.900	2.980	3.005	3.010	3.030	3.035	3.090	3.095

Kurowski method, was located at 2840 m (Table 2). Prior to this time, Saz and Creus (2001) and Saz (2003) detected in dendroclimatic reconstructions of temperature data series in northern Spain a long and negative trend beginning in the middle of the 18th century. In agreement, and also favoring glacial growth, the dendroclimatic reconstruction of Capdella analyzed in this paper indicates that in the 1810s decade, summer and annual temperatures were lower than those of the reference period 1951–1980 (0.25 °C and 0.35 °C lower, respectively), while total annual precipitation was higher.

4.2. Glacial stabilization period (1820–1830 to 1857)

Between 1820–1830 and 1857, Maladeta Glacier shows a clear stabilization. Although the contact of the ice terminus with the frontal portion of the LIA moraine was lost in some areas (Figs. 3 and 7), the glacier morphology remained almost unchanged. The glacier had a surface extent of 148.5 ha, registering a rate of surface-loss since the previous stage of just -0.11 ha year^{-1} (Table 2). This glacial stabilization period might be related to annual and summer temperatures which were below the mean of the reference period and similar to those of the previous analyzed stage. Precipitation, on the contrary, is mainly below the average of the reference period, at least until the beginning of the 1850s decade. This cold and dry phase has been identified in Spain (Barriendos, 1996; Saz, 2003) as well as in other areas of Europe (Jacoby and D'Arrigo, 1989; Pfister, 1992; Tarussov, 1992; Serre-Bachet, 1994; Briffa, 1995; Koslowski and Glaser, 1995, 1999; Kalela-Brundin, 1999).

4.3. Marked glacial depletion period (1857 to 1901–1904)

The first period of marked ice depletion in the Maladeta Glacier during the last two centuries was at the second half of the 19th century (1857 to 1901–1904). In 1876, the glacier began to show signs of degradation (Figs. 3 and 8; Table 2), confirmed from photographic evidence from 1901–1904 (Figs. 3 and 9; Table 2). Between 1857 and 1901–1904, the glacier lost almost one third of its surface area (47.8 ha), with a rate of surface loss during this period of -1.03 ha year^{-1}. In fact, several works indicate that the LIA had already ended in Europe by this time (Gribbin and Lamb, 1979; Jacoby and D'Arrigo, 1989; Jones et al., 1998; Mann et al., 1999). Our dendroclimatic reconstruction shows that summer temperatures were 0.3 °C and annual temperatures 0.2 °C higher in the 1860s and 1870s decades than those of the reference period, whereas winter and annual precipitation were approximately 10% lower. These unfavourable climatic conditions could be responsible for the high rate of surface loss in the glacier. In the 1880s and 1890s, temperature was slightly colder or around the mean of the reference period, but precipitation was still reduced, particularly winter precipitation, which only on four

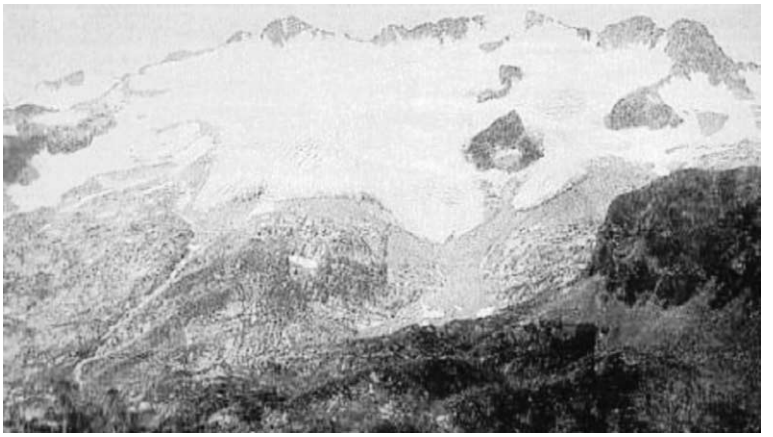

Fig. 7. View of Maladeta Glacier from Puerto de Benasque (Photo: A. Civiale; Date: 1857).

Fig. 8. Panoramic view of Maladeta Glacier from Puerto de Benasque (Photo: E. Trutat; Date: 1876).

occasions between 1878 and 1908 surpassed the mean value of the 1951–1980 period.

4.4. Moderated glacial depletion period (1901–1904 to 1914–1920)

The rate of glacial depletion diminished during the first two decades of the 20th century (−0.55 ha year^{-1}). The Maladeta Glacier, around 100 years after the LIA maximum, had a surface area of 92.9 ha (60.9% of the LIA maximum value); retreat of its ice front terminus was considerable, and the glacier had a length of 1340 m, 220 m shorter than the length measured in 1820–1830 (Figs. 3 and 10; Table 2). During this period, following the trend detected in the last two decades of 19th century, temperature was still mainly below the reference period, but precipitation was also reduced, with a mean decrease of approximately 20% in winter precipitation and 9.4% in annual precipitation for 1898–1908, and 22.6% and 6.6%, respectively, for 1914–1920.

4.5. Glacial stabilization period (1914–1920 to 1934–1935)

The tendency towards stabilization continued and culminated in this period, registering a rate of ice surface loss of just −0.18 ha year^{-1}. The glacier had a surface area of 89.7 ha (58.8% of the initial area) but showed almost no changes in length or maximum and minimum ice altitudes (Figs. 3 and 11; Table 2). The stabilization could be related in this case to both precipitation and temperature values which lie near to the mean of the reference period. The only cold peaks identified fall within the interval 1929–1932 (0.4 °C below the reference period for summer, and 0.21 °C for annual temperature).

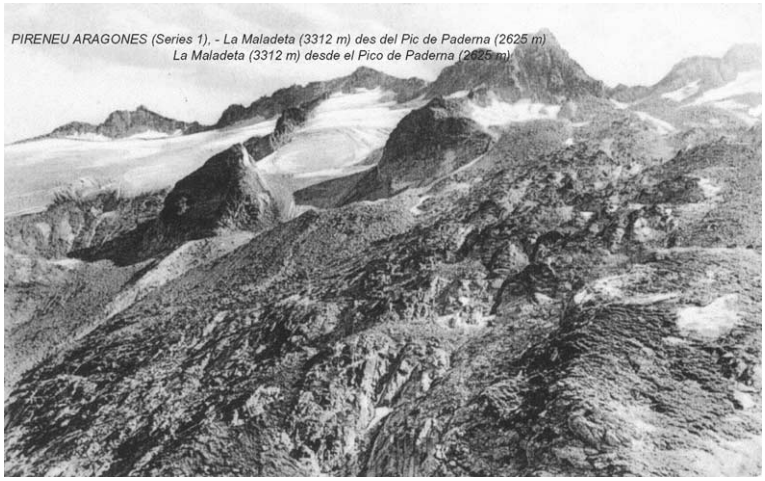

Fig. 9. View of Maladeta Glacier central-western sector (Photo: J. Soler Santaló; Date: 1901).

Fig. 10. Panoramic view of Aneto (left) and Maladeta (right) glaciers from Puerto de la Picada (Photo: C. Lana Sarrate; Date: 1920).

4.6. Moderated glacial depletion period (1934–1935 to 1957)

Glacial depletion increases during these two decades, with a rate of surface loss of −0.68 ha year^{-1}. The ice body had an extent of 74.2 ha (48.7% of the LIA maximum), with a length of approximately 1220 m (Fig. 3; Table 2). This surface and length diminution might be related to the warm anomaly detected in the second half of the 1940s, with summer and annual temperature 0.25 °C and 0.4 °C, respectively, above the mean of the reference period. Precipitation during the 1940s is below the mean, with decreases in winter precipitation of 10% and 8% in the annual values.

4.7. Glacial stabilization period (1957 to 1981)

A noticeable stabilization in the deglaciation process is registered in the Maladeta Glacier during this period. The rate of surface-loss since the previous stage is just −0.13 ha year^{-1} (Fig. 3; Table 2), almost as low as the one calculated for the post-LIA maximum in the first half of the 19th century. The glacial body lost only 3.3 ha during these 24 years; its length, maximum and minimum ice elevation and ELA altitude did not show significant variations. The reason for this stabilization is clear, and lies in prolonged summer and annual temperature values well below the mean of the reference period, and on winter and annual precipitation values

Fig. 11. Panoramic view (from left to right) of Aneto, Maladeta and Alba glaciers from Puerto de Benasque (Photo: L. García Sainz; Date: 1935).

Fig. 12. Detailed view of the Maladeta Glacier separation into the two present ice bodies: right, Maladeta Occidental Glacier; left, Maladeta Oriental Glacier (Photo: J. Chueca; Date: 1995).

above that mean, particularly during the 1960s decade.

4.8. Marked glacial depletion period (1981 to 2000)

The climate during the last two decades has been particularly damaging for Maladeta Glacier. The rate of surface loss between 1981 and 1990 (−1.03 ha year^{-1}) was practically an order of magnitude greater than that measured during the previous phase, and similar to that mentioned for the period 1857 to 1901–1904, in the beginning of the deglaciation process after the LIA maximum. Between 1990 and 2000, the rate of surface loss remained high (−0.88 ha year^{-1}) and during that decade fragmentation of the glacier into the current two bodies (Maladeta Occidental and Maladeta Oriental Glaciers) ocurred (Figs. 3, 12, 13 and 14; Table 2). The two climatic variables analyzed in our study continued to have a strong influence on glacier evolution: The 1980s and 1990s were two of

Fig. 13. Detailed view of Maladeta Occidental Glacier (Photo: J. Camins; Date: 1992).

Fig. 14. View of Maladeta Occidental and Oriental glaciers from Puerto de Benasque (Photo: J. Camins; Date: 1999).

the most warm and dry periods of the last two centuries. Temperature (annual and, particularly, summer temperature), surpassed almost constantly the mean of the reference period, with peaks 1.1 °C and 2.0 °C above the mean, respectively, while winter and annual precipitation were almost always below average.

In order to further investigate the relative roles of temperature and precipitation in the observed glacier variations, a correlation analysis between climatic data and glacier surface loss rate (GSL) was undertaken. The analysis was made using data from the nine reconstructed stages (1820–1830/1857; 1857/1876; 1876/1901–1904; 1901–1904/1914–1920; 1914–1920/1934–1935; 1934–1935/1957; 1957/1981; 1981/1990; 1990/2000), measuring for each period the strength of the linear relationship between GSL and the average of the standardized values for third trimester temperature, annual temperature, first trimester precipitation and annual precipitation (Table 3).

The results show the existence of statistically significant correlation between annual temperature and GSL (correlation coefficient $r=-0.68$; $\alpha=0.05$), and between winter precipitation and GSL (correlation coefficient $r=0.59$; $\alpha=0.10$). No significant relation was found between summer temperatures and GSL (correlation coefficient $r=-0.49$) or annual precipitation and GSL (correlation coefficient $r=0.47$). The results obtained are not conclusive, considering the small number of stages used in the correlation analysis and the difficulty of properly evaluating (due to the nature of the data sets) the response time between climate fluctuations and GSL. They could be indicative of the importance of annual temperature and winter precipitation as the main control on glacier development in a temperate mid-latitude Mediterranean alpine context such as the Pyrenees, where precipitation in the form of snow is almost limited to the winter period and high temperatures are not only typical of the summer months, but can be registered from early spring to late autumn.

Table 3
Glacier ice wastage and climatic data for the nine analyzed periods

	GSL	T3	TA	P1	PA
1820–1830/1857	−0.11	−0.43	−0.43	0.14	0.04
1857/1876	−0.97	−0.12	−0.05	0.20	0.20
1876/1901–1904	−1.03	−0.34	−0.26	−0.06	0.25
1901–1904/1914–1920	−0.55	−0.53	−0.41	−0.04	0.25
1914–1920/1934–1935	−0.18	−0.31	−0.31	0.10	0.11
1934–1935/1957	−0.68	0.25	−0.18	0.23	0.02
1957/1981	−0.13	0.05	−0.61	0.55	0.51
1981/1990	−1.03	1.52	0.64	−0.67	−0.62
1990/2000	−0.88	0.67	0.66	−0.80	−0.32

GSL: glacier surface loss rate (ha $year^{-1}$); T3: average of the standardized values for third trimester temperature; TA: average of the standardized values for annual temperature; P1: average of the standardized values for first trimester precipitation; PA: average of the standardized values for annual precipitation.

5. Conclusions

Maladeta Glacier represents a fine example to test the relationship between climate and glacier fluctuations. The deglaciation process that all Pyrenean glaciers have undergone since the Little Ice Age is evident here: From having an area of 152.3 ha in 1820–1830, the glacier has been reduced to merely 54.5 ha in 2000 (total extent of the present two ice bodies), a 35.7% reduction of the initial surface area. This ice depletion value is in accord with those mentioned by Chueca et al. (2002) for the remainder of the main South-Pyrenean glaciated areas: 32.0% for the whole Maladeta massif, 39.2% for Posets, 24.9% for Taillon-Monte Perdido, and 33.6% for Infiernos-Punta Zarra.

The results obtained reveal also that the ELA of Maladeta Glacier increased 255 m between 1820–1830 and 2000. This evolution is in keeping with the trend observed in other alpine Mediterranean glaciers, which have experienced a constant rise of their equilibrium line altitudes during 19th and 20th centuries, as well as associated and prolonged periods of negative mass balances. This has been the case in the small glaciers of the Southern Maritime Alps (Gellatly et al., 1994a; Pappalardo, 1999), the Central Apennines with the Ghiacciaio del Calderone (Gellatly et al., 1994b; D'Orefice et al., 2000), the Sierra Nevada with the Corral del Veleta Glacier (Messerli, 1980; Gómez Ortiz and Salvador, 1997), and on the northern, climatically Atlantic and more humid Pyrenees (Gellatly et al., 1995; René, 2000). The timing of this deglaciation process is not the same in all alpine Mediterranean areas, due to the importance of local factors such as topography, shading, presence or absence of debris-cover or particular topoclimatic conditions, but the general tendency towards reduction of the surface area and thickness, or even glacier extinction, is well evidenced at this macro regional level.

A noticeable matter observed in Maladeta Glacier is that the periods during which the climate favoured positive mass balances saw only stabilization of ice volume and surface area losses, but were insufficient to interrupt the general recessional trend. No advances of the ice front have been recorded or documented during the whole deglaciation process. The fact that many current Pyrenean glaciers, due to their steep topographic positioning, lack a cover of debris on their surfaces which would reduce ablation, is contributing to the process.

Finally, a minimum response time of very few years seems to exist between temperature and precipitation changes and the stabilization or retreat of the Maladeta Glacier. As the lag time for a glacier to react to climatic fluctuations depends mainly on its size and its latitudinal location, climatic changes, even subdued ones, are felt more precisely by smaller glaciers placed in warmer settings (such as the Pyrenean) than by larger glaciers in higher latitudinal areas. This fact makes the Pyrenean glacial remnants useful and reliable proxy indicators to analyze the impact of the current climatic changes on mid-latitude mountains.

Acknowledgements

Financial support for this study was provided by the following research projects: 'Estudio de la dinámica de los glaciares del Pirineo aragonés' (H-9007-2001) funded by the Gobierno de Aragón; 'Precipitaciones y temperaturas de la mitad septentrional española a partir del siglo XVII. Reconstrucciones dendroclimáticas' (CLI96-1862) funded by CICYT; and 'Estudio de la dinámica glaciar en el Pirineo español en el contexto del cambio climático: correlación con reconstrucciones dendroclimáticas termo-pluviométricas' (UZ2002-HUM-01) funded by Zaragoza University.

References

Aniol, R.W., 1983. Tree-ring analysis using CATRAS. Dendrochronologia 1, 45–53.

Barriendos, M., 1996. El clima histórico de Catalunya (siglos XIV–XIX). Fuentes, métodos y primeros resultados. Rev. Geogr., 69–96.

Briffa, K.R., 1995. Interpreting high-resolution proxy climate data: the example of dendroclimatology. In: Von Storch, H., Navarra, A. (Eds.), Analysis of Climate Variability: Applications of Statistical Techniques. Springer, Berlin, pp. 77–94.

Chueca, J., Julián, A., 1994. El medio natural de la Alta Ribagorza: macizo de la Maladeta. Col. Naturalia, Madrid (155 pp.).

Chueca, J., Julián, A., 1996. Datación de depósitos morrénicos de la Pequeña Edad del Hielo: macizo de la Maladeta. In: Pérez

Alberti, A., Martini, P., Chesworth, W., Martínez Cortizas, A. (Eds.), Dinámica y Evolución de Medios Cuaternarios. Xunta de Galicia, Santiago de Compostela, pp. 171–182.

Chueca, J., Julián, A., 2002. Los glaciares pirenaicos aragoneses: estudio de su evolución desde el final de la Pequeña Edad del Hielo hasta la actualidad a través de documentación fotográfica. Diputación de Huesca, Huesca (323 pp.).

Chueca, J., Julián, A., Peña, J.L., 2002. Comparación de la situación de los glaciares del Pirineo español entre el final de la Pequeña Edad del Hielo y la actualidad. Bol. Glaciol. Aragon. 3, 13–41.

Chueca, J., Julián, A., López, I., 2003. Variations of Glaciar Coronas, Pyrenees, Spain, during the 20th century. J. Glaciol. 49 (166), 449–455.

Cook, E.R., Kairiukstis, L.A. (Eds.), 1990. Methods of Dendrochronology. Kluwer Academic Publishers, London (394 pp.).

Copons, R., Bordonau, J., 1997. El registro glaciar correspondiente a la Pequeña Edad del Hielo en la Península Ibérica. In: Ibáñez, J.J., Valero, B.L., Machado, C. (Eds.), El paisaje mediterráneo a través del espacio y del tiempo. Implicaciones en la desertificación. Geoforma Ediciones, Logroño, pp. 295–310.

Creus, J., Fernández, A., 1992. Cuantificación del clima pasado a partir de series dendrocronológicas. Coloquio Geogr. Cuantit., 393–407.

Creus, J., Génova, M., Fernández, A., Pérez, A., 1992. New dendrocrhonologies for Spanish Mediterranean zone. Lunqua 34, 76–78.

D'Orefice, M., Pecci, M., Smiraglia, C., Ventura, R., 2000. Retreat of Mediterranean glaciers since the Little Ice Age: case study of Ghiacciaio del Calderone, Central Apennines, Italy. Arct. Antarct. Alp. Res. 32 (2), 197–201.

Fritts, H., 1990. Modelling tree-ring and environmental relationships for dendrochronological analisys. In: Dixon, C. (Ed.), Forest Growth Process Modeling of Responses to Environmental Stress. Timers Press, Oregon, pp. 360–382.

Fritts, H., 1991. Reconstructing large-scale climatic patterns from tree-ring data. University of Arizona Press, Tucson (286 pp.).

Fritts, H., Shaskin, A.V., 1995. Modelling tree-ring structure as related to temperature, precipitation and day-length. In: Lewis, T.E. (Ed.), Tree-Rings as Indicators of Ecosystem Health. CRC, Boca-Raton, pp. 17–57.

Gellatly, A.F., Grove, J.M., Latham, R., Parkinson, R.J., 1994a. Observations of the glaciers in the Southern Maritime Alps (Italy). Rev. Géomorphol. Dyn. 43 (3), 93–107.

Gellatly, A.F., Smiraglia, C., Grove, J.M., Latham, R., 1994b. Recent variations of Ghiacciaio del Calderone, Abruzzi, Italy. J. Glaciol. 40 (136), 486–490.

Gellatly, A.F., Grove, J.M., Bücher, A., Latham, R., Whalley, W.B., 1995. Recent historical fluctuations of the Glacier du Taillon, Pyrénées. Phys. Geogr. 15 (5), 399–413.

Gómez Ortiz, A., Salvador, F., 1997. El glaciarismo de Sierra Nevada, el más meridional de Europa. In: Gómez Ortiz, A., Pérez Alberti, A. (Eds.), Las huellas glaciares de las montañas españolas. Universidade de Santiago de Compostela, Santiago de Compostela, pp. 385–430.

Gribbin, J., Lamb, H.H., 1979. Climatic change in historical times. In: Gribbin, J. (Ed.), Climatic Change. Cambridge University Press, Cambridge, pp. 68–82.

Guiot, J., 1990. Methods of calibration. In: Cook, E.R., Kairiukstis, L.A. (Eds.), Methods of Dendrochronology. Kluwer Academic Publishers, London, pp. 165–172.

Holmes, R., 1997. The Dendrochronology Program Library. The International Tree Ring Data Bank Program. Laboratory of Tree-Ring Research. University of Arizona, Tucson, pp. 40–74.

Jacoby, G.C., D'Arrigo, R., 1989. Reconstructed Northern Hemisphere annual temperature since 1671 based on high latitude tree ring data from North America. Clim. Change 14, 39–59.

Joanne, A., 1862. Itinéraire général de la France. Les Pyrénées. Hachette, Paris (767 pp.).

Jones, P.D., Briffa, K.R., Barnett, T.P., Tett, S.F.B., 1998. High resolution paleoclimatic records for the last millennium: interpretation, integration an comparison with General Circulation Model control-run temperatures. Holocene 8 (4), 455–471.

Julián, A., Chueca, J., 1998. Le Petit Âge Glaciaire dans les Pyrénées Centrales Méridionales: estimation des paléotempératures à partir d'inférences géomorphologiques. Sud-Ouest Eur. 3, 79–88.

Kalela-Brundin, M., 1999. Climatic information from tree-rings of *Pinus sylvestris* L. and a reconstruction of summer temperatures back to AD 1500 in Femundsmarka, eastern Norway, using partial least squares regression (PLS) analysis. Holocene 9 (1), 59–77.

Koslowski, G., Glaser, R., 1995. Reconstruction of the ice winter severity since 1701 in the western baltic. Clim. Change 31, 79–98.

Koslowski, G., Glaser, R., 1999. Variations in reconstructed ice winter severity in the western baltic from 1501 to 1995, and their implications for the North Atlantic oscillation. Clim. Change 41, 175–191.

Mann, M.E., Bradley, R.S., Hughes, M.K., 1999. Northern Hemisphere temperatures during the past millennium: inferences, uncertainties, and limitations. Geophys. Res. Lett. 26, 759–762.

Martínez, R., García, F., 1994. Trabajos de glaciología en el glaciar de la Maladeta. Campaña 1991–92. In: MOPTMA (Ed.), La nieve en las cordilleras españolas. Ministerio de Obras Públicas, Transporte y Medio Ambiente, Madrid, pp. 209–236.

Martínez, R., García, F., Macheret, Y., Navarro, J., Bisbal, L., 1997. El sustrato subglaciar y la estructura interna de los glaciares del Aneto y la Maladeta cartografiados por geo-radar de ultra-alta frecuencia (UHF). In: MMA (Ed.), La nieve en las cordilleras españolas. Ministerio de Medio Ambiente, Madrid, pp. 227–249.

Martínez de Pisón, E., Arenillas, M., 1988. Los glaciares actuales del Pirineo español. In: MOPU (Ed.), La nieve en el Pirineo español. Ministerio de Obras Públicas y Urbanismo, Madrid, pp. 29–98.

Messerli, B., 1980. Mountain glaciers in the Mediterranean area and in Africa. World Glacier Inventory Workshop Publication, vol. 126, pp. 197–211.

Packe, C., 1867. A Guide to Pyrenees. Longmans Green and Co., London (301 pp.).

Pappalardo, M., 1999. Remarks upon the present-day condition of the glaciers in the Italian Maritime Alps. Geogr. Fis. Din. Quat. 22, 79–82.

Parrot, F., 1823. Reise in den Pyrenäen. G. Reiner, Berlin (145 pp.).
Pfister, C., 1992. Monthly temperature and precipitation in central Europe 1525–1979. In: Bradley, R.S., Jones, P.D. (Eds.), Climate Since A.D. 1500. Routledge, London, pp. 118–142.
René, P., 2000. Etat des lieux des glaciers des Pyrénées françaises. Compte rendu de la campagne de terrain (septembre 1999). Société Hydrotechnique de France, Grenoble (16 pp.).
Saz, M.A., 2003. Análisis de la evolución del clima en la mitad septentrional de España desde el siglo XV a partir de series dendroclimáticas. Servicio de Publicaciones de la Universidad de Zaragoza, Zaragoza (1105 pp.).
Saz, M.A., Creus, J., 2001. El clima del Pirineo centro-oriental desde el siglo XV: estudio dendroclimático del observatorio de Capdella. Bol. Glaciol. Aragon. 2, 37–79.
Schrader, F., 1894. Sur l'etendue des glaciers des Pyrénées. Annuaire Club Alpine Français 21, 403–423.
Serre-Bachet, F., 1994. Annual and summer mean temperature reconstructions from tree rings in western and southern Europe since A.D. 1500 with special reference to the late Maunder Minimum. In: Frenzel, B. (Ed.), Climatic Trends and Anomalies in Europe 1675–1715. European Science Foundation, Strasbourg, pp. 265–274.
Tarussov, A., 1992. The artic from Svalbard to Severnaya Zemlya: climatic reconstructions from ice cores. In: Bradley, R.S., Jones, P.D. (Eds.), Climate Since A.D. 1500. Routledge, London, pp. 505–516.